

# Metallicity in damped Lyman- $\alpha$ systems: evolution or bias?

N. Prantzos and S. Boissier

*Institut d’Astrophysique de Paris, 98bis, Bd. Arago, 75104 Paris*

## ABSTRACT

Assuming that damped Lyman- $\alpha$  (DLA) systems are galactic discs, we calculate the corresponding evolution of metal abundances. We use detailed multi-zone models of galactic chemical evolution (reproducing successfully the observed properties of disc galaxies) and appropriate statistics (including geometrical probability factors) to calculate the average metallicity as a function of redshift. The results are compatible with available observations, *provided that observational biases are taken into account*, as suggested by Boissé et al. (1998). In particular, high column density *and* high metallicity systems are not detected because the light of background quasars is severely extinguished, while low column density *and* low metallicity systems are not detectable through their absorption lines by current surveys. We show that these observational constraints lead to a “no-evolution” picture for the DLA metallicity, which does not allow to draw strong conclusions about the nature of those systems or about their role in “cosmic chemical evolution”.

**Key words:** Galaxies: general - evolution - spirals - photometry - abundances

## 1 INTRODUCTION

Damped Lyman- $\alpha$  systems (DLAs) are high column density ( $N(\text{HI}) > 10^{20} \text{ cm}^{-2}$ ) absorbers detected in the optical spectra of quasars up to relatively high redshifts (up to  $z \sim 5$ ). Their study constitutes a powerful means to investigate the properties of distant galaxies (or of their building blocks). In particular, DLA metal abundances have been widely used in the past few years (e.g. Prochaska and Wolfe 1999, Pettini et al. 1999, Edmunds and Philips 1997, and references therein) in order to probe the nature of DLAs (i.e. galactic discs vs. galaxies of other morphological types) or even to probe the so-called “cosmic chemical evolution” (i.e. the global evolution of gas, metallicity and star formation rate in the Universe). It is not clear, however, whether the observed abundances alone allow to probe the nature or the history of those systems. One reason is possible depletion of metals into dust (e.g. Pei and Fall 1995). In this work we investigate another factor, namely observational biases, along the lines suggested by Boissé et al. (1998). Assuming that (proto)galactic discs constitute a quite plausible model for such systems we show that observational biases may completely alter our interpretation of DLA metal abundances.

## 2 OBSERVATIONAL BIASES OF METAL ABUNDANCE ESTIMATES IN DLAS

In Fig. 1 we present the empirical evidence on which this work is based. Observations of Zn abundances in DLAs ob-

tained by several groups are plotted as a function of HI column density  $N(\text{HI})$ . This plot is an up-dated version of Fig. 19 of Boissé et al. (1998) and confirms the suggestion of those authors, namely that there seems to be an anti-correlation between the observed Zn abundance and  $N(\text{HI})$ , independently of redshift  $z$ . As Boissé et al. (1998) notice, this is not to be interpreted as a physical correlation (i.e. that high metallicities are characteristic of low column density systems); indeed, the observed abundance gradients in spiral galaxies offer clear evidence that higher abundances are found in the inner disc, where gas column densities are also higher (e.g. Garnett et al. 1997).

The correlation of Fig. 1 is rather to be interpreted in terms of observational biases: no systems with a combination of metallicity and column density outside the shaded region of Fig. 1 are presently detected, *even if such systems do exist*. The lack of high metallicity *and* high column density systems should be attributed to extinction effects, since extinction depends on both those factors. The lack of low metallicity *and* low column density systems is attributed by Boissé et al. (1998) again to observational selection effects, i.e. to the fact that below some level the amount of Zn atoms along the line of sight is insufficient to allow for a proper spectroscopic detection.

How “realistic” are these empirically determined detectability constraints and how can they be quantitatively understood? We postpone a discussion of those matters to Sec. 4. We simply wish to illustrate here the effect of these

constraints (assuming they are real) on the detectability of a Milky Way type disc through its metal absorption lines.

In a recent work (Boissier and Prantzos 1999, hereafter BP99) we presented a detailed model for the chemical and spectrophotometric evolution of the disc of our Galaxy. The galactic disc is simulated as an ensemble of concentric, independently evolving rings, gradually built up by infall of primordial composition. The chemical evolution of each zone is followed by solving the appropriate set of integro-differential equations. The spectrophotometric evolution is followed in a self-consistent way, i.e. with the star formation rate  $\Psi(t)$  and metallicity  $Z(t)$  of each zone determined by the chemical evolution, and the same stellar Initial Mass Function (from Kroupa et al. 1993). The adopted stellar yields, lifetimes, evolutionary tracks and spectra are metallicity dependent. Dust absorption is included according to the prescriptions of Guiderdoni et al. (1998) and assuming a “sandwich” configuration for the stars and dust layers (Calzetti et al. 1994). The star formation rate (SFR) is locally given by a Schmidt-type law, i.e. proportional to some power of the gas surface density  $\Sigma_g$  and varies with galactocentric radius  $R$  as:

$$\Psi(t, R) = \alpha \Sigma_g(t, R)^{1.5} V(R) R^{-1} \quad (1)$$

where  $V(R)$  is the circular velocity at radius  $R$ . This radial dependence of the SFR is suggested by the theory of star formation induced by density waves in spiral galaxies (e.g. Wyse and Silk 1989).

It turns out that the number of observables reproduced by the model is much larger than the number of free parameters. In particular the model reproduces present day “global” properties (amount of gas, SFR, and supernova rates), as well as the current Milky Way disc luminosities in various wavelength bands and the corresponding radial profiles of gas, stars, SFR and metal abundances; moreover, the adopted inside-out star forming scheme leads to a scale-length of  $\sim 4$  kpc in the B-band and  $\sim 2.8$  kpc in the K-band, in agreement with observations (see BP99).

At this point it should be noticed that, among all metals observed in DLAs through absorption line measurements, Zn is usually considered to be the most reliable tracer of metallicity, because its abundance is expected to suffer little from depletion into dust (e.g. Pettini et al. 1997). However, from the theoretical point of view, the nucleosynthesis of Zn is not well understood. The only known production site is massive stars, and the most detailed models of this site are those of Woosley and Weaver (1995, WW95), who give the only available models with yields of the various isotopes as a function of initial stellar metallicity. The Zn yields of these models show an unexplained behaviour: the dominant Zn isotope,  $^{64}\text{Zn}$ , is underproduced, while the yields of the next two more important isotopes,  $^{66}\text{Zn}$  and  $^{68}\text{Zn}$ , increase strongly as metallicity increases from  $0.1 Z_\odot$  to  $Z_\odot$ . The reason for this behaviour in the models is not yet well understood. As a result, the  $[\text{Zn}/\text{Fe}]$  ratio calculated with the metallicity dependent yields of WW95 and a chemical evolution model shows a rather abrupt and pronounced increase for metallicities  $[\text{Fe}/\text{H}] > -1$ , while it stays nearly constant at lower metallicities (Timmes et al. 1995a, Goswami and Prantzos 2000). This behaviour is not found in the observed pattern of the Zn/Fe ratio: both halo and disk stars of all metallicities show solar Zn/Fe (see Goswami and Prantzos 2000 and references therein), despite the fact that SNIa, the

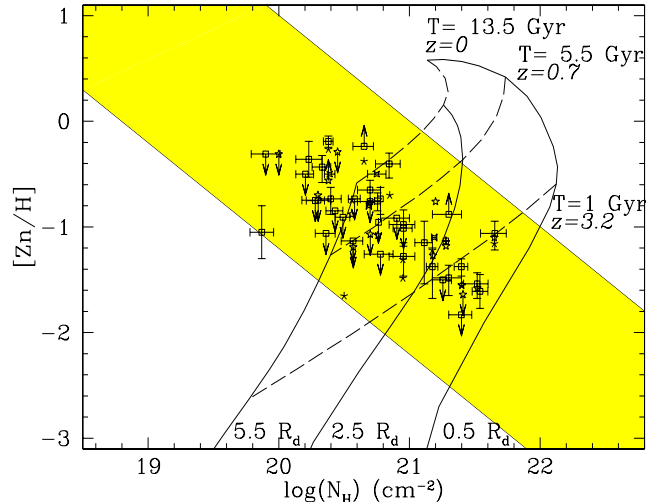


**Figure 1.** Zn abundances vs gas column density  $N(\text{HI})$ . Observations in DLAs are from Pettini et al. (1994, 1997, 1999), Prochaska and Wolfe (1999), Boissé et al. (1998), Lu et al. (1996). Observations are apparently contained within the *shaded area*, which is limited by  $[\text{Zn}/\text{H}] + \log(N(\text{HI})) < 21$  (*upper diagonal*) and  $[\text{Zn}/\text{H}] + \log(N(\text{HI})) > 18.8$  (*lower diagonal*). For illustration purposes, we show the evolution of Zn vs gas column density in three different zones of a Milky Way type disc (*solid curves*, at 0.5, 2.5 and 5.5 scalelengths from the center, respectively) according to our models. The column densities correspond to our model disc seen “face-on”. The disc evolves from the lower left to the upper right in this diagram, as can be seen from the 3 isochrones (*dashed curves*) at times  $T=1$  Gyr, 5.5 Gyr and 13.5 Gyr, respectively; the corresponding redshifts are for a cosmological model with  $H_0=65 \text{ km/s/Mpc}$ ,  $\Omega_0=0.3$  and a galaxy formation redshift  $z=6$  (i.e. the time of formation of the first stars).

main Fe producers in the disk, do not produce significant Zn amounts.

This situation does not allow us to trust theoretical nucleosynthesis prescriptions for the evolution of Zn, since theory seems unable to reproduce observations in the Galaxy. Therefore we adopt an empirical approach for the nucleosynthesis of Zn, already suggested in Timmes et al. (1995b): based on the observed Zn/Fe pattern in the Galaxy, we assume that Zn traces Fe at all metallicities. Since the history of Fe in the Galaxy is observationally well constrained (at least in the solar neighborhood) and reasonably well reproduced by our models (see BP99), we assume that it can be safely used to trace the history of Zn in other places as well.

In Fig. 1 we present the evolution of the Zn abundance in three representative zones of the Milky Way model (corresponding to the inner disc, the solar neighborhood and the outer disc, respectively) as a function of the corresponding gas column densities of those zones. It should be noticed that in our models we do not distinguish between atomic and molecular gas and the curves in Fig. 1 are drawn by assuming that all the gas is in atomic form (the contribution of He, i.e. 10% by number, is properly removed). This approximation certainly affects the results (i.e. the curve corresponding to the inner disc, where most of the gas is known to be in molecular form, should be shifted to the left by 0.5 on that same scale), but for our illustration purposes the figure is quite appropriate.

Indeed, it is clearly seen that the actual chemical evolution of the disc cannot be revealed by observations, because of the empirically determined constraints discussed previously. At any given epoch (i.e. along the “isochrones” in Fig. 1) only a sub-sample of the disc can be probed. At early times this sub-sample is representative of the inner regions which reach rapidly relatively high column densities and moderate metallicities; at late times these regions develop such high densities *and* metallicities that they move into the “forbidden” part of the diagram (upper right). At late times then, it is the outer regions that can be probed through the absorption lines.

Obviously, in such conditions it is difficult to derive the real chemical history of the system, since only snapshots of *different regions at different times* can be available, not of the same regions at different times.

### 3 METALLICITY EVOLUTION IN DLAS

The discussion in the previous section suggests that our picture of DLA chemical evolution, obtained through quasar absorption line measurements, may be seriously biased. Indeed, if taken at face value, Fig. 1 suggests that at early times the lowest metallicities and at late times the highest metallicities are unobservable. Could this bias modify the picture to such an extent as to give the impression of no-evolution at all?

In order to answer quantitatively this question, a working model for the evolution of DLAs is needed. Some authors suggested that DLAs are proto-galactic discs (e.g. Prochaska and Wolfe 1996, Ferrini et al. 1997, Prantzos and Silk 1998) while others interpreted them as low surface brightness galaxies (Jimenez et al., 1998), dwarf irregulars (Matteucci et al. 1997), galactic halos (Valageas et al. 1999) or proto-galactic “building blocks” (Haehnelt et al. 1998, Ledoux et al. 1998). It has also been suggested that DLAs differ substantially from the galaxies that contribute mostly to the observed SFR in the Universe (e.g. Pettini et al. 1999).

We shall adopt in this work the hypothesis that DLAs are galactic discs. We shall use a detailed model we developed recently for the chemical and spectrophotometric evolution of galactic discs (Boissier and Prantzos 2000). It is essentially the Milky Way model presented in Sec. 2, extended to disc galaxies through “scaling properties” derived by Mo, Mao and White (1998) in the framework of the Cold Dark Matter (CDM) scenario for galaxy formation. In our simplified version of this scenario disc profiles can be expressed in terms of only two parameters: maximal rotational velocity  $V_C$  (measuring the mass of the halo and, by assuming a constant halo/disc mass ratio, also the mass of the disc) and spin parameter  $\lambda$  (measuring the specific angular momentum of the halo). If all discs are assumed to start forming their stars at the same time (but not at the same rate!), the profile of a given disc can be expressed in terms of the one of our Galaxy. We constructed a grid of 25 models characterised by  $V_C = 80, 150, 220, 290, 360$  km/s and  $\lambda/\lambda_{MW} = 1/3, 1, 5/3, 7/3, 3$ , respectively, where  $\lambda_{MW}$  is the spin parameter of the Milky Way. Increasing values of  $V_C$  correspond to more massive discs and increasing values of  $\lambda$  to more extended ones. The SFR is calculated from Eq.

1, with the appropriate velocity profile  $V(R)$ . Notice that the efficiency  $\alpha$  is not a free parameter, since it is the same as in the Milky Way model.

It turns out that this simple model reproduces fairly well most of the main properties of present days discs (Boissier and Prantzos 2000): disc sizes and central surface brightness, Tully-Fisher relations in various wavelength bands, colour-colour and colour-magnitude relations, gas fractions vs. magnitudes and colours, abundances vs. local and integrated properties, as well as integrated spectra for different galactic rotational velocities. Moreover, as shown in Prantzos and Boissier (2000), it also reproduces the observed abundance gradients in disc galaxies.

In Fig. 2 we present the results of our models for the Zn evolution in DLAs (assumed to be galactic discs) as a function of redshift  $z$ . For clarity, only the evolution of the inner and outer disc is presented in each panel (*thin curves*, corresponding to zones located at 0.5 and 5.5 scalelengths from the centre, respectively). Star formation is assumed to start at redshift  $z=6$  for all discs, but any value of  $z > 4.5$  would produce results similar to those displayed here. The resulting evolution is not very different from that calculated in e.g. Prantzos and Silk (1998) for the Milky Way, or in Ferrini et al. (1997) with multi-zone disc models. Notice that Malaney and Chaboyer (1996), Timmes et al. (1995b), Matteucci et al. (1997), Edmunds and Philipps (1997) and Lindner et al. (1999) have studied metallicity evolution in DLAs with one-zone models, differing by the star formation timescales or by the time of the beginning of star formation.

It can be clearly seen in Fig. 2 that between redshifts  $z \sim 3$  and  $z \sim 1$  there is substantial metallicity evolution in all galactic zones, typically an increase by a factor  $\sim 10$ . Such an increase is certainly not observed in the available data, which is also displayed on each one of the panels in Fig. 2.

The region enclosed within *thick solid curves* in Fig. 2 is obtained by application of the “empirical constraints” of Fig. 1, i.e. by excluding all regions with a combination of metallicity and column density  $F(\text{Zn}, \text{N(HI)}) = [\text{Zn}/\text{H}] + \log(\text{N(HI)})$  such that  $F < 18.8$  or  $F > 21$ . The resulting observational picture is now completely different from the real one: no sizeable evolution in metallicity is observed (except, perhaps, in the lowest redshift range, where metallicities are somewhat higher than average).

It should be noticed that the empirical “filter” has been applied to our models by assuming that discs are seen “face-on” and that all the gas is in the form of HI. These simplifying assumptions have opposite effects on the derived column density along the line of sight: adopting a different inclination would increase the column density of our disc models; taking into account that part of the gas is in the form of H<sub>2</sub>, would decrease it. The former factor can be treated statistically, but not the latter. Taking all other uncertainties into account (i.e. possible variations in the H<sub>2</sub>/HI ratio with metallicity, see Combes 1999) we think that Fig. 2 gives a rather good first approximation to the real situation.

The results of Fig. 2 are summarised in the upper panel of Fig. 3, where we plot in the same diagram all the “filtered” zones of our models as a function of redshift (*shaded area*) and compare them to observations. The “no-evolution” picture is even more clearly seen now, especially in the  $z \sim 1$ –3 redshift range. A firm prediction of these models is that the Zn abundances of DLAs at higher redshifts, in the range

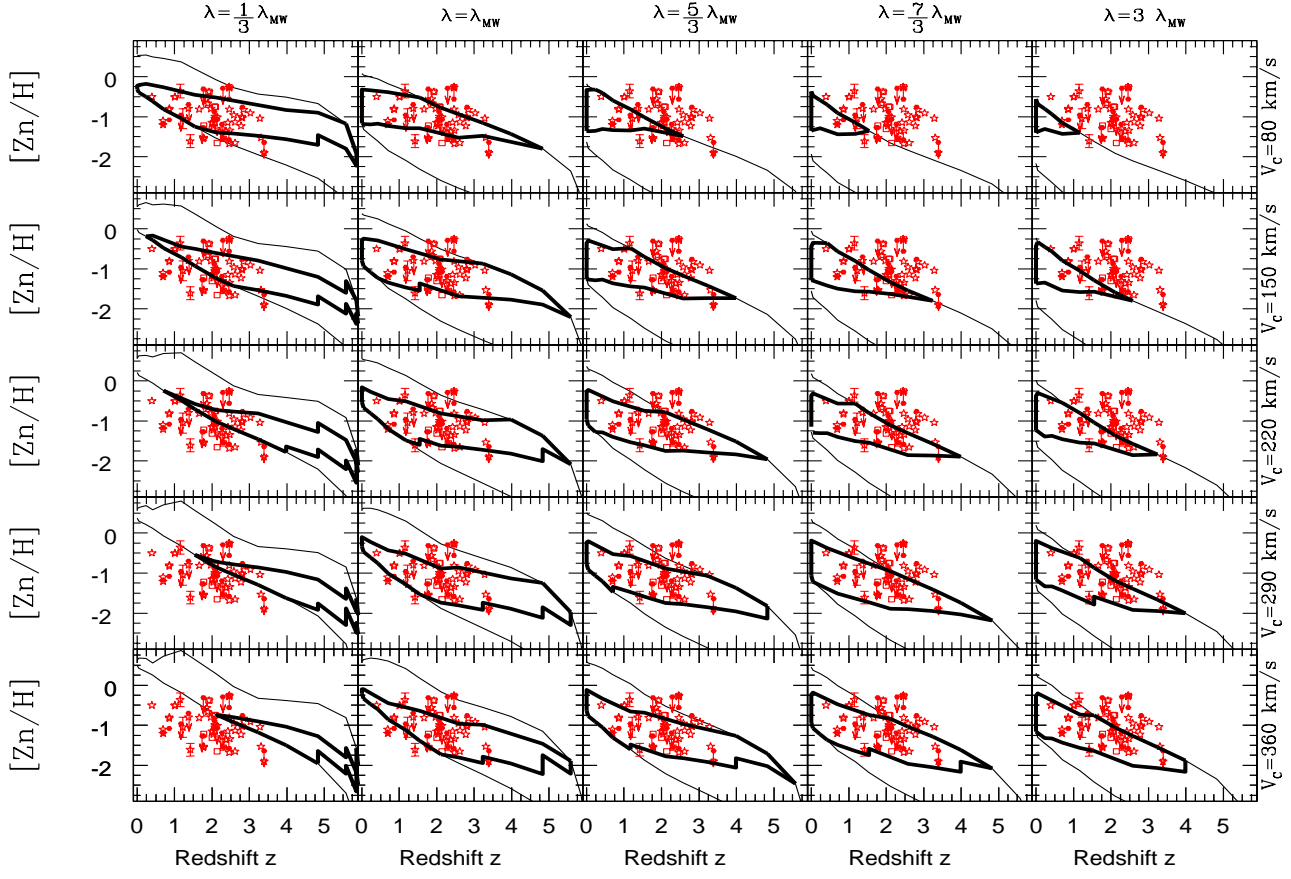


**Figure 2.** Evolution of Zn abundances in our models as a function of redshift  $z$ . Results are presented for a grid of 25 disc models, characterised by 5 values of the disc maximal circular velocity  $V_C$  (80, 150, 220, 290, 360 km/s, *from top to bottom*) and 5 values of the spin parameter  $\lambda/\lambda_{MW}$  (1/3, 1, 5/3, 7/3, 3, *from left to right*) where  $\lambda_{MW}$  is the corresponding value for the Milky Way disc. For clarity, only the evolution of two “extreme” zones is shown for each model, at 0.5 and 5.5 scalelengths from the center (*upper and lower curve*, respectively, in each panel), which span the evolution of the whole disc. The region enclosed within *thick curves* is obtained by application of the empirical selection criterion of Fig. 1 (i.e.  $18.8 < [\text{Zn}/\text{H}] + \log(\text{N(HI)}) < 21$ ), assuming that all discs are seen “face-on”. It can be seen that this “filter” selects zones within a restricted range of  $[\text{Zn}/\text{H}]$  value (independently of redshift), and leads to a no-evolution picture. Observations (the same in all panels) are from the references listed in the legend of Fig. 1.

$z \sim 3-5$ , will be not too different from those already detected at  $z \sim 1-3$ .

Assuming that this first approximation is correct (i.e. that DLAs are indeed galactic discs) it is interesting to calculate the *most probable metallicity values* expected at a given redshift. Even if our basic assumptions are correct, this is by no means a trivial task, since it implies the knowledge of the appropriate statistical factors as a function of the redshift. For illustration purposes we adopt here the following simplified assumptions:

i) the distribution function of discs in the velocity space  $V_C$  is time-independent and given by the expression suggested in Gonzalez et al. 1999 (in the following we simplify, for clarity, the notation  $V_C$  to  $V$ , unless if explicitly stated otherwise):

$$F_V(V)dV = \tilde{\Psi}_* \left( \frac{V}{V_*} \right)^\beta \exp \left[ - \left( \frac{V}{V_*} \right)^n \right] \frac{dV}{V_*}. \quad (2)$$

The parameters  $\Psi_*$ ,  $V_*$ ,  $\beta$  and  $n$  are determined in Gonzalez et al. (1999) on the basis of observed Tully-Fisher relationships and luminosity (Schechter-type) functions. We

adopt here the set of parameters of their Table 4 (fifth row, LCRS-Courteau data) corresponding to the velocity interval covered by our models. Our results would not be affected much by the choice of another velocity function, since the form of  $F_V$  always favours discs of low  $V$ .

ii) the distribution function in spin parameter  $\lambda$ -space is time-independent and given by:

$$F_\lambda(\lambda)d\lambda = \frac{1}{\sqrt{2\pi}\sigma_\lambda} \exp \left[ -\frac{\ln^2(\lambda/\bar{\lambda})}{2\sigma_\lambda^2} \right] \frac{d\lambda}{\lambda} \quad (3)$$

with  $\bar{\lambda}=0.05$  and  $\sigma_\lambda=0.5$  (obtained by numerical simulations, see e.g. Mo, Mao and White, 1998) and  $\lambda_{MW}=0.06$  for the Milky Way disc (Sommer-Larsen, private communication). The  $\lambda$ -function favours moderately “compact” discs (those with  $\lambda \sim 0.04-0.05$ ).

iii) the probability that a line of sight to a QSO intercepts a disc in the radius interval  $[R, R+dR]$  is proportional to the geometrical cross-section  $F_R dR = 2\pi R dR$ , favouring the detection of the outer regions of the larger discs.

iv) the distributions  $F_V$ ,  $F_\lambda$  and  $F_R$  are independent. Applying the joint probability function  $F(V, \lambda, R) =$

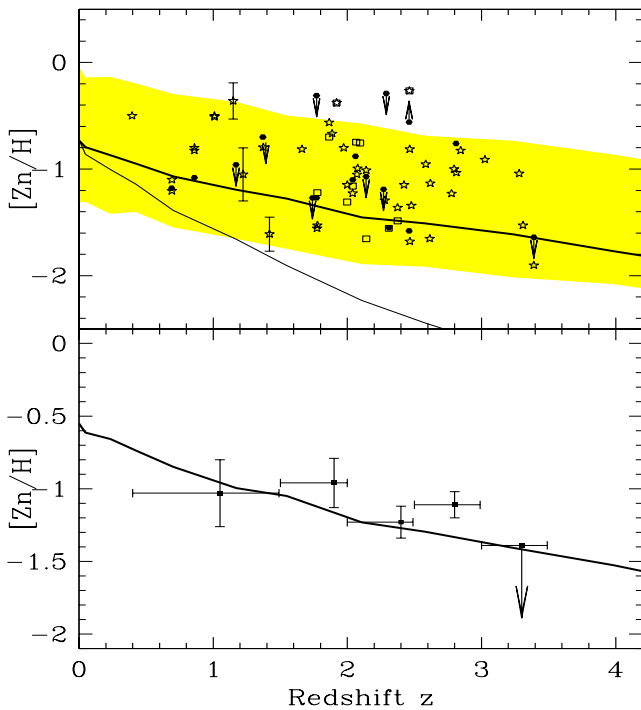


**Figure 3.** Evolution of mean metallicities of our disc galaxy models as a function of redshift  $z$ . *Upper panel:* The thin curve is the mean metallicity of all the zones of our models, i.e. the “unfiltered” value  $\langle [Zn/H] \rangle_U$  obtained with  $\Phi(R)=1$  always in Eq. (4); the thick curve is the mean value  $\langle [Zn/H] \rangle_F$  of the zones “filtered” through the empirical constraint of Fig. 1, i.e. the mean value of the shaded area, obtained with  $\Phi(R)=1$  for those filtered zones and  $\Phi(R)=0$  for the others. The shaded area includes all the “filtered” zones of our models, i.e. all the zones inside thick curves in Fig. 2. Observations are as in Fig. 2. *Lower panel:* Column density weighted average metallicity of the “filtered zones”  $\langle [Zn/H] \rangle_{FW}$ , obtained by Eq. (5) (thick curve); data are from Pettini et al. (1999).

$F_V F_\lambda F_R$  to our models, we obtain the mean metallicities  $\langle [Zn/H] \rangle$  shown in Fig. 3. The two curves in the upper panel are obtained by:

$$\left\langle \left[ \frac{Zn}{H} \right] \right\rangle = \frac{\int_{\lambda} \int_V \int_0^{R_L} F(\lambda, V, R) \Phi(R) \left[ \frac{Zn}{H}(R) \right] dR dV d\lambda}{\int_{\lambda} \int_V \int_0^{R_L} F(\lambda, V, R) \Phi(R) dR dV d\lambda} \quad (4)$$

where  $R_L$  is the radius of the largest disc in our models. The mean value over the whole disc (i.e. without applying the empirical “filter”) corresponds to  $\Phi(R)=1$  in all zones and is given by the thin curve in Fig. 3. In that case,  $\langle [Zn/H] \rangle_U$  ( $U$  for “Unfiltered”) increases by a factor  $\sim 20$  between redshifts  $z=3$  and  $z=1$  and is clearly below all observational data (because the outer, low metallicity, regions of the discs are favoured in that case). This shows the importance of properly taking into account various statistical factors, something that has not been done in previous studies of DLAs with multi-zone disc models (e.g. in Ferrini et al. 1997 and Prantzos and Silk 1998).

The mean value  $\langle [Zn/H] \rangle_F$  over the “filtered” disc zones (i.e. those in the shaded area of Fig. 3) is obtained with  $\Phi(R)=1$  in those zones and  $\Phi(R)=0$  outside them. It is

shown by the thick curve in Fig. 3. This  $\langle [Zn/H] \rangle_F$  value is in the lower range of the “filtered” values, again because of the geometrical factor  $F_R$ .  $\langle [Zn/H] \rangle_F$  increases by a factor of  $\sim 2$  between  $z=3$  and  $z=1$ , an increase which is compatible with the observations.

Pettini et al. (1999) have also estimated the column density weighted average of the  $[Zn/H]$  values in DLAs, by binning their data in 5 redshift bins (the last bin, at  $z > 3$ , being in fact an upper limit only). Again, no substantial evolution is seen in the data (*lower panel* in Fig. 3). We also calculated the corresponding average metallicity in our models, by folding with the gas column densities  $N_H(R)$  of the “filtered” zones (assuming that all but 10 % by number - corresponding to He - is in the form of atomic hydrogen):

$$\left\langle \left[ \frac{Zn}{H} \right] \right\rangle_{FW} = \frac{\int_{\lambda} \int_V \int_0^{R_L} F(\lambda, V, R) \Phi \left[ \frac{Zn}{H} \right] N_H dR dV d\lambda}{\int_{\lambda} \int_V \int_0^{R_L} F(\lambda, V, R) \Phi N_H dR dV d\lambda} \quad (5)$$

where  $\Phi$ ,  $[Zn/H]$  and  $N_H$  depend on radius  $R$ . The resulting evolution is shown in the lower panel of Fig. 3. It can be seen that the weighted mean metallicity  $\langle [Zn/H] \rangle_{FW}$  of the “filtered” zones of our models evolves in a way which is certainly compatible with the data. A clear prediction of the model is that at low redshifts ( $z < 1$ ) there should be as much evolution as in the  $z=1-3$  range (i.e. a factor of  $\sim 2-3$  increase in the weighted mean metallicity of DLAs in both cases).

In summary, by using a self-consistent model of galactic chemical evolution (i.e. reproducing in detail the properties of local galaxies) and incorporating “reasonable” statistics and appropriate empirical constraints, we have shown unambiguously that only a small degree of evolution should be expected for the observed mean metallicity of DLAs; according to our models, these systems may well be galactic discs.

#### 4 ORIGIN OF BIASES

It is interesting to see how the empirically determined upper limit in the  $Zn$  vs  $N(\text{HI})$  plane may be interpreted in terms of extinction. We shall assume here that our model discs constitute gaseous screens, seen face-on and reducing the intensity of the light of background quasars. The corresponding extinction is calculated in the rest-frame of the absorber by the formula:

$$A_\lambda(z) = (A_\lambda/A_V)_\odot (A_V/N_H)_\odot N_H (Z/Z_\odot)^{1.6} \quad (6)$$

where  $(A_\lambda/A_V)_\odot$  is the local normalised extinction curve (Natta and Panagia, 1984),  $(A_V/N_H)_\odot$  is the extinction in the V-band in the solar neighborhood (from Bohlin et al., 1978) and the exponent 1.6 in the metallicity term is introduced in order to reproduce the observed extinction curves in the Small and Large Magellanic Clouds (Guiderdoni and Rocca-Volmerange, 1987). The wavelength  $\lambda$  depends on the redshift  $z$  of the absorber. Since the background QSO light is observed in the visible ( $\lambda_{V,obs}=0.55 \mu$ ), we have for the corresponding wavelength  $\lambda_{ABS}$  of the absorber

$$\lambda_{ABS}(z) = \frac{\lambda_{V,obs}}{1+z} \quad (7)$$

For illustration purposes, we calculated the extinction at 3 different redshifts  $z=1,2,3$  (i.e. in the absorber’s rest-

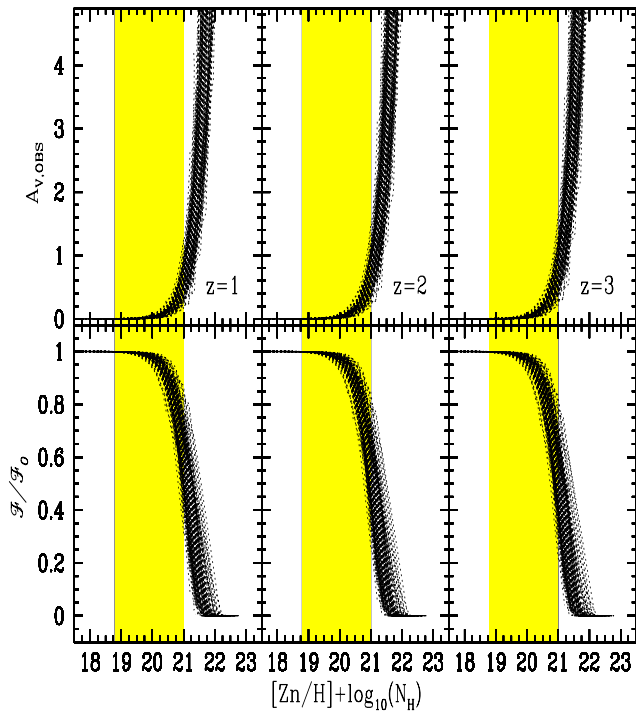


**Figure 4.** *Upper panel:* Extinction  $A_v$  of background light caused by the various zones of our models, assumed to be gaseous screens (seen face-on) at redshift  $z=1,2,3$  (from left to right, respectively) of column density  $N(H)$  and metallicity  $[Zn/H]$  (Eq. 6). *Lower panel:* Corresponding reduction factor in the brightness of the background light. In both panels the shaded area corresponds to the one of Fig. 1, i.e. satisfying the “filter”  $18.8 < [Zn/H] + \log(N(H)) < 21$ . It is clearly seen that extinction increases rapidly to the right of the upper limit, presumably making the background QSOs unobservable.

frame  $\lambda_{ABS} = 0.275, 0.183$  and  $0.137 \mu$ , respectively) during the evolution of all the zones of our models. We plot it in Fig. 4 as a function of  $F = [Zn/H] + \log(N(H))$  (*upper panel*), while in the lower panel we plot the corresponding fraction of background light filtered through the screen. It can be seen that for values of  $F > 21$  (i.e. above the empirically determined limit in Fig. 1) extinction increases rapidly, reaching 1 mag at  $z=1$ , 1.5 mag at  $z=2$  and 2 mag at  $z=3$ . The background intensity drops below 40% of its initial value. Our results substantiate the claim of Boissé et al. (1998) that extinction is biasing the interpretation of metallicity abundance determinations in DLAs.

As for the lower value of the “empirical” constraint, it can be understood as follows: Taking into account that, by definition, DLAs correspond to column densities  $\log(N(H)) > 20$ , the lower limit  $F < 18.8$  corresponds to  $[Zn/H] < -1$ , i.e. to less than  $5 \times 10^{11}$  atoms of Zn per  $\text{cm}^2$  along the line of sight (adopting a solar ratio  $(\text{Zn}/\text{H})_{\odot} \sim 4.5 \times 10^{-8}$  by number, e.g. Anders and Grevesse 1989). Current surveys of DLAs typically reach  $N(\text{Zn}) > 10^{12} \text{ cm}^{-2}$  (Pettini et al. 1997), which explains, perhaps, why the lower left part of Fig. 1 is void.

In any case, it should be interesting to detect the stellar population responsible for the chemical enrichment of the gas in DLAs. In Fig. 5 we plot our model B-V values of

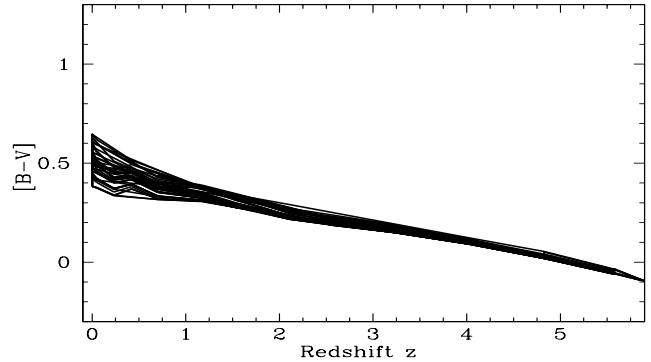


**Figure 5.** B-V vs. redshift for the stellar populations of the disc zones of our models that satisfy the condition  $18.8 < [Zn/H] + \log(N(\text{HI})) < 21$  (corresponding to the shaded area of Fig. 3). Discs are assumed to be seen “face-on”; inclined discs should provide higher B-V values.

that population, which span a narrow range  $0.2 < B-V < 0.4$  for redshifts  $1 < z < 3$ . In fact, these values are lower limits, since our model discs are assumed to be seen face-on. Thus, one of the firm predictions of our model applied to DLAs is that the underlying stellar population should be somewhat redder than the curve in Fig. 4.

## 5 SUMMARY

The observational constraint  $18.8 < [Zn/H] + \log(N(\text{HI})) < 21$  (Boissé et al. 1998) has profound implications for the interpretation of metal abundances detected in DLAs. Assuming that DLAs are galactic discs, and using detailed (and successful) models for disc evolution, we show that current observations cannot probe the true evolution of those systems: a no-evolution picture, compatible with available data, emerges when the empirical constraints are taken into account. We calculate average metallicities in the galactic zones of our models that are “filtered” by the empirical constraints, by taking into account appropriate statistical factors. We find that the resulting column density weighted average metallicity shows a small increase at low redshifts and is compatible with currently available data. These findings suggest that DLAs may well be galactic discs, as argued e.g. in Prochaska and Wolfe, 1999 (for a different view, see Pettini et al., 1999).

We also show quantitatively how extinction may be indeed responsible for the non-detection of metal rich DLAs of high column density, as suggested by Boissé et al. (1998); according to those authors, such DLAs may be one day detected in samples drawn from the observation of fainter QSOs, independently of the redshift. Moreover, metal poor DLAs of low column density should also be detected with more sensitive instruments. Finally, if our interpretation of currently observed DLAs as galactic discs is correct, we expect that the underlying stellar populations should have  $B-V > 0.2$  (by a small amount) in the redshift range  $1 < z < 3$ .

**Acknowledgements:** We are grateful to Patrick Boissé and Patrick Petitjean for useful discussions and comments on this work.

## REFERENCES

Anders E. & Grevesse N., 1989, *Geochimica and Cosmochimica Acta*, 53, 197

Bohlin R., Savage B. & Drake J., 1978, *ApJ*, 224, 132

Boissé P., Le Brun V., Bergeron J. & Deharveng J.-M., 1998, *A&A*, 333, 841

Boissier S. & Prantzos N., 1999, *MNRAS*, 307, 857 (BP99)

Boissier S. & Prantzos N., 2000, *MNRAS* in press and astro-ph/9909120 (BP2000)

Calzetti D., Kinney A. & Storchi-Bergmann T., 1994, *ApJ*, 429, 582

Combes F., 1999, in "H<sub>2</sub> in Space", Cambridge University Press, ed. F. Combes and G. Pineau des Forets (astro-ph/9910296)

Edmunds M. G. & Phillips S., 1997, *MNRAS*, 292, 733

Ferrini F., Molla M. & Díaz A. I., 1997, *ApJ*, 487, L29

Garnett D., Shields G., Skillman E., Sagan S. & Dufour R., 1997, *ApJ*, 489, 63

Gonzales A., Williams K., Bullock J., Kolatt T. and Primack J., 1999, To appear in *ApJ*, astro-ph/9908075

Goswami A. & Prantzos N., 2000, *A&A*, submitted

Guiderdoni B. & Rocca-Volmerange B., 1987, *A&A*, 186, 1

Guiderdoni B., Hivon E., Bouchet R. & Maffei B., 1998, *MNRAS*, 295, 877

Haehnelt M., Steinmetz M., Rausch M., 1998, *ApJ*, 495, 647

Jimenez R., Padoan P., Matteucci F. & Heavens A., 1998, *MNRAS*, 299, 123

Kroupa P., Tout C. & Gilmore G., 1993, *MNRAS*, 262, 545

Ledoux C., Petitjean P., Bergeron J., Wampler E. J., Srianand R., 1998, *A&A*, 337, 51

Lindner U., Fritze-Von Alvensleben U. & Fricke K., 1999, *A&A*, 341, 709

Lu L., Sargent W., Barlow T., Churchill C. & Vogt S., 1996, *ApJ Suppl.*, 107, 475

Malaney R. & Chaboyer, 1996, *ApJ*, 462, 57

Matteucci F., Molaro P. & Vladilo G., 1997, *A&A*, 321, 45

Mo H., Mao S. & White S., 1998, *MNRAS*, 295, 319

Natta A. & Panagia N., 1984, *ApJ*, 287, 228

Pei Y. & Fall S., 1995, *ApJ*, 454, 69

Pettini S., Smith L., Hunstead R. & King D., 1994, *ApJ*, 426, 79

Pettini S., Smith L., King D. & Hunstead R., 1997, *ApJ*, 486, 665

Pettini S., Ellison S., Steidel C. & Bowen D., 1999, *ApJ*, 510, 576

Prantzos N. & Silk J., 1998, *ApJ*, 507, 229

Prantzos N. & Boissier S., 2000, *MNRAS* in press and astro-ph/9911111

Prochaska J. & Wolfe A., 1996, *ApJ*, 470, 403

Prochaska J. & Wolfe A., 1999, *ApJ Suppl.*, 121, 369

Timmes F., Woosley S. & Weaver T., 1995a, *ApJ*, 458, 617

Timmes F., Lauroesch J. & Truran J., 1995b, *ApJ*, 451, 468

Valageas P., Schaeffer R. & Silk J., 1999, *A&A*, 691, 711

Wyse R. & Silk J., 1989, *ApJ*, 339, 700